

X-ray structure of the dimeric bis[(1,7-dicarba-*closo*-dodecaborane-1-carboxylato)-di-*n*-butyltin] oxide [☆]

Marcel Gielen ^{a,*}, Abdeslam Bouhdid ^a, Rudolph Willem ^{a,b}, Vladimir I. Bregadze ^c,
Lidia V. Ermanson ^c, Edward R.T. Tiekink ^d

^a Department of General and Organic Chemistry, Faculty of Applied Sciences, Free University of Brussels (V.U.B.), Pleinlaan 2, B-1050 Brussels, Belgium

^b High Resolution NMR Centre, Free University of Brussels (V.U.B.), Pleinlaan 2, B-1050 Brussels, Belgium

^c Institute of Organo-Element Compounds, Russian Academy of Sciences, Vavilova 28, INEOS, Moscow, V334, 117813, GSP-1, Russia

^d Department of Chemistry, The University of Adelaide, Adelaide, S.A. 5005, Australia

Received 26 April 1995

Abstract

X-ray diffraction studies reveal the structure of $\{[(1,7-C_2B_{10}H_{11}-1-COO)Bu_2Sn]_2O\}_2$ to be analogous to most other $\{[RCOO)Bu_2Sn]_2O\}_2$ compounds. The dimer features a central $Bu_4Sn_2O_2$ unit with the two Bu_2Sn groups being linked via bridging oxygen atoms, each of which also carries an exocyclic Bu_2Sn moiety. The two pairs of exo- and endo-cyclic tin atoms are each linked via a symmetrically bridging carboxylate ligand and the two remaining ligands coordinate the exocyclic tin atom only, in the monodentate mode. The *in vitro* anti-tumour activity of this compound, against a variety of cell lines, is compared with those of clinically used compounds.

Keywords: Anticancer; Carborane; Carboxylate; Nuclear magnetic resonance; Stannyl; Tin

1. Introduction

The anti-tumour activity of many compounds of the type $\{[RCOO)Bu_2Sn]_2O\}_2$ has been determined against two human tumour cell lines, MCF-7, a mammary tumour, and WiDr, a colon carcinoma [1–5]. The compounds were in general quite active *in vitro*. For instance, the di-*n*-butyltin monofluorobenzoates have ID_{50} values approximately half those of etoposide [1]. The 2,3-difluorobenzoate is even more active than the monofluorobenzoates against MCF-7 with an ID_{50} value comparable to that of mitomycin C. The ID_{50} value of the corresponding 2,3,6-trifluorobenzoate is of the same order of magnitude while that of the 2,3,4,5-tetrafluorobenzoate is lower. Against the WiDr cell line, all fluorobenzoates exhibit comparable activities with $\{[(2, 3-$

$F_2C_6H_2CO_2)Bu_2Sn]_2O\}_2$ being the significantly most active [2].

As a continuation of our study on organotin carboxylates, we report here the synthesis, spectral characterisation, X-ray structure and *in vitro* anti-tumour activity of a di-*n*-butyltin *m*-carborane-1-carboxylate, $\{[(1,7-C_2B_{10}H_{11}-1-COO)Bu_2Sn]_2O\}_2$. It belongs to a novel class of organotin compounds involving a carboranecarboxylate ligand.

2. Results and discussion

2.1. Synthesis

X-ray quality crystals of the new di-*n*-butyltin *m*-carborane-1-carboxylate were obtained from a 1:1 condensation of dibutyltin(IV) oxide with *m*-carborane-1-carboxylic acid and its structure has been determined by spectroscopic and X-ray diffraction methods. The ¹H,

[☆] Dedicated to Prof. Dr. Herbert Schumann on the occasion of his 60th birthday.

* Corresponding author.

^{13}C and ^{119}Sn NMR spectra of the compound displayed the usual duplicate resonances for the different types of Bu_2Sn moieties, characteristic for the dimeric dicarboxylatotetra-organodistannoxanes, $\{[(\text{R}'\text{COO})\text{R}_2\text{Sn}]_2\text{O}\}_2[1-5]$.

2.2. Crystal and molecular structures of $\{[(1,7\text{-C}_2\text{B}_{10}\text{H}_{11}\text{-1-COO})\text{Bu}_2\text{Sn}]_2\text{O}\}_2$

The molecular structure of $\{[(1,7\text{-C}_2\text{B}_{10}\text{H}_{11}\text{-1-COO})\text{Bu}_2\text{Sn}]_2\text{O}\}_2$, illustrated in Fig. 1, shows that the structure is similar to those of a majority of analogous $\{[\text{RCOO})\text{Bu}_2\text{Sn}]_2\text{O}\}_2$ compounds [6]; selected interatomic parameters are collected in Table 1. There is disorder in the structure, in particular associated with the butyl groups (see Section 3). In Fig. 1 only one position of each of the disordered atoms is shown for reasons of clarity; in Table 1, all parameters associated with the C(21) atoms, i.e. C(21a) and C(21b), are listed. The structure is molecular, without any significant intermolecular contacts in the lattice; the closest nonhydrogen contact of 3.12(2) Å occurs between the O(5) and C(5') atoms (symmetry operation 1-x, -1-y, 1-z).

The structure is centrosymmetric about a $\text{Bu}_4\text{Sn}_2\text{O}_2$ core. Attached to each bridging oxygen atom is an exocyclic Bu_2Sn unit leading to a three-coordinate O(1) atom. Further connections between the tin atoms arise as a result of bridging carboxylate ligands which form experimentally equivalent Sn-O bonds distances to the endo- and exo-cyclic tin atoms, i.e. Sn(1)-O(2) 2.236(9) Å and Sn(2)-O(3) 2.24(1) Å. The remaining independent carboxylate ligand coordinates in the monodentate mode to the exocyclic tin atom exclusively with Sn(2)-O(4) 2.192(8) Å. This configuration leads to five coordinate tin centres, each existing in a distorted trigonal bipyramidal geometry. The trigonal plane about the Sn(1) atom is defined by the O(1), C(11) and C(15) atoms with the axial positions being occupied by the

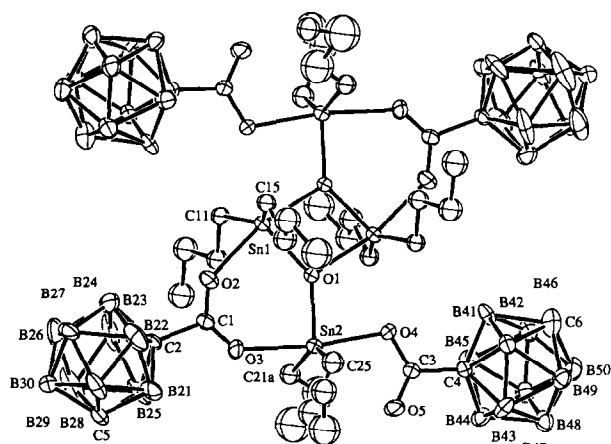


Fig. 1. Molecular structure and crystallographic numbering scheme for $\{[(1,7\text{-C}_2\text{B}_{10}\text{H}_{11}\text{-1-COO})\text{Bu}_2\text{Sn}]_2\text{O}\}_2$.

Table 1

Selected interatomic distances (Å) and angles (°) for $\{[(1,7\text{-C}_2\text{B}_{10}\text{H}_{11}\text{-1-COO})\text{Bu}_2\text{Sn}]_2\text{O}\}_2$

Sn-O(1)	2.025(7)	Sn(1)-O(1') ^a	2.165(7)
Sn(1)-O(2)	2.236(9)	Sn(1)-C(11)	2.11(1)
Sn(1)-C(15)	2.15(1)	Sn(2)-O(1)	1.987(7)
Sn(2)-O(3)	2.24(1)	Sn(2)-O(4)	2.192(8)
Sn(2)-C(21a) ^b	2.26(4)	Sn(2)-C(21b) ^b	2.02(3)
Sn(2)-C(25)	2.15(2)	C(1)-O(2)	1.19(2)
C(1)-O(3)	1.17(2)	C(3)-O(4)	1.26(1)
C(3)-O(5)	1.20(1)	C(1)-C(2)	1.55(2)
C(3)-C(4)	1.55(2)		
O(1)-Sn(1)-O(1')	77.4(3)	O(1)-Sn(1)-O(2)	89.2(3)
O(1)-Sn(1)-C(11)	107.5(4)	O(1)-Sn(1)-C(15)	109.6(4)
O(1')-Sn(1)-O(2)	166.6(3)	O(1')-Sn(1)-C(11)	98.0(4)
O(1')-Sn(1)-C(15)	95.8(4)	O(2)-Sn(1)-C(11)	86.6(5)
O(2)-Sn(1)-C(15)	88.0(5)	C(11)-Sn(1)-C(15)	142.3(5)
O(1)-Sn(2)-O(3)	91.0(3)	O(1)-Sn(2)-O(4)	80.7(3)
O(1)-Sn(2)-C(21a)	105.2(9)	O(1)-Sn(2)-C(21b)	123(1)
O(1)-Sn(2)-C(25)	107.9(5)	O(3)-Sn(2)-O(4)	171.1(4)
O(3)-Sn(2)-C(21a)	85(1)	O(3)-Sn(2)-C(21b)	78(1)
O(3)-Sn(2)-C(25)	89.2(5)	O(4)-Sn(2)-C(21a)	94(1)
O(4)-Sn(2)-C(21b)	103(1)	O(4)-Sn(2)-C(25)	96.6(5)
C(21a)-Sn(2)-C(25)	128(1)	Sn(1)-O(1)-Sn(1')	102.6(3)
Sn(1)-O(1)-Sn(2)	137.0(4)	Sn(1)-O(1')-Sn(2')	120.4(4)
Sn(1)-O(2)-C(1)	138(1)	Sn(2)-O(3)-C(1)	136(1)
Sn(2)-O(4)-C(3)	108.4(8)	O(2)-C(1)-O(3)	127(2)
O(2)-C(1)-C(2)	115(2)	O(3)-C(1)-C(2)	118(1)
O(4)-C(3)-C(5)	124(1)	O(4)-C(3)-C(4)	117(1)
O(5)-C(3)-C(4)	119(1)		

^a Primed atoms are related by a crystallographic centre of inversion,

^b The C(21) atom is disordered over two sites with site occupancy = 0.5.

O(1') and O(2) atoms [O(1')-Sn(1)-O(2) 166.6(3)°]; the Sn(1) atom lies 0.083(1) Å out of this plane in the direction of the O(1) atom. For the Sn(2) atom, the trigonal plane is defined by the O(1), C(25) and C(21a) [or C(21b)] atoms and the axial positions are occupied by the O(3) and O(4) atoms; O(3)-Sn(2)-O(4) 171.1(4)°. For the trigonal plane containing the C(21a) atom, the Sn(2) atom lies 0.079(1) Å out of the plane in the direction of the O(4) atom, the corresponding deviation for the C(21b) atom is 0.153(1) Å. Distortions from the ideal geometries may be traced, in part, to the presence of close intramolecular Sn...O interactions. Thus, the centrosymmetrically related O(4') atom forms a contact of 2.746(8) Å with the Sn(1) atom, which opens up the C(11)-Sn(1)-C(15) angle to 142.3(5)° from the ideal angle of 120°. Similarly, an interaction of 2.85(1) Å between the Sn(2) and O(5) atoms results in the expansion of the C(25)-Sn(2)-C(21a) and C(25)-Sn(2)-C(21b) angles to 146(1) and 128(1)°, respectively; however, the disorder associated with the C(21) position complicates the situation. Whereas the intramolecular Sn...O contacts mentioned above are well within the van der Waals distances for these atoms, the relatively large separations and the minor perturbations from the ideal trigonal bipyramidal geometries indicate that these in-

teractions must be considered as weak. The molecular structure for $\{[(1,7\text{-C}_2\text{B}_{10}\text{H}_{11}\text{-1-COO})\text{Bu}_2\text{Sn}]_2\text{O}\}_2$ conforms to the common structural motif found for compounds with the general formula $\{[(\text{R}'\text{COO})\text{R}_2\text{Sn}]_2\text{O}\}_2$. Other variations from the major motif involve different coordination modes of the carboxylate ligands and may lead to different coordination geometries/numbers at tin [6].

2.3. In vitro anti-tumour activities

The compound $\{[(1,7\text{-C}_2\text{B}_{10}\text{H}_{11}\text{-1-COO})\text{Bu}_2\text{Sn}]_2\text{O}\}_2$ was screened in vitro against six tumoural cell lines of human origin. The ID_{50} values obtained, in ng ml^{-1} , are summarised in Table 2.

Against these cell lines, $\{[(1,7\text{-C}_2\text{B}_{10}\text{H}_{11}\text{-1-COO})\text{Bu}_2\text{Sn}]_2\text{O}\}_2$ is somewhat less active than methotrexate and doxorubicin. Compound **1** is more active than 5-fluorouracil, *cis*-platin and carboplatin. This places the anti-tumour activity of the present compounds in an intermediate category.

3. Experimental

3.1. Synthesis and purification

Bis-[(1,7-dicarbaclosododecaborane-1-carboxylato)-di-*n*-butyl tin] oxide, $\{[(1,7\text{-C}_2\text{B}_{10}\text{H}_{11}\text{-1-COO})\text{Bu}_2\text{Sn}]_2\text{O}\}_2$, was synthesised in benzene (150 ml) from di-*n*-butyltin oxide (664 mg) and the corresponding organic acid (500 mg). *m*-Carborane-1-carboxylic acid was prepared following Grimes [7] by the action of an equimolar amount of *n*-butyl lithium to *m*-carborane followed by the carboxylation of the obtained 1-lithio-*m*-carborane with CO_2 and acid hydrolysis.

After 20 min of reflux, a clear solution was obtained which was then refluxed for a further 5 h. The binary azeotrope water/benzene was distilled off with a Dean-Stark funnel. The obtained benzene solution was distilled to 50% of its initial volume and the remaining solvent was evaporated in vacuo. The solid obtained

was purified by recrystallisation from methylene chloride/*n*-hexane. Yield: 82%; m.p.: 230–233 °C.

3.2. Structure determination of $\{[(1,7\text{-C}_2\text{B}_{10}\text{H}_{11}\text{-1-COO})\text{Bu}_2\text{Sn}]_2\text{O}\}_2$

Intensity data for a colourless crystal ($0.03 \times 0.16 \times 0.16$ mm) were measured at room temperature on a Rigaku AFC6R diffractometer fitted with Mo- $\text{K}\alpha$ radiation (graphite monochromator, $\lambda = 0.71073 \text{ \AA}$) using the $\omega:2\theta$ scan technique. No decomposition of the crystal occurred during the data collection, the data set was corrected for Lorentz and polarisation effects [8] and for absorption employing an empirical procedure [9]. Of the 10 392 data collected, 9970 were unique and of these 3233 satisfied the $I \geq 3.0\sigma(I)$ criterion of observability and were used in the subsequent analysis.

Crystal data for $\text{C}_{44}\text{H}_{116}\text{B}_{40}\text{O}_{10}\text{Sn}_4$: $M = 1712.6$, triclinic, space group $P\bar{1}$, $a = 13.666(5)$, $b = 14.036(5)$, $c = 13.531(4)$, $\alpha = 108.21(3)$, $\beta = 110.52(3)$, $\gamma = 104.07(3)^\circ$, $V = 2119(1) \text{ \AA}^3$, $Z = 1$ (tetramer), $D_{\text{expt}} = 1.341 \text{ g cm}^{-3}$, $m = 12.08 \text{ cm}^{-1}$.

The structure was solved by direct methods [10] and refined by a full-matrix least-squares procedure based on F [8]. The nonhydrogen, nonbutyl atoms were refined with anisotropic thermal parameters. Considerable disorder was detected for the butyl groups with the C(21) atom being refined over two sites with equal occupancy and the C(24) and C(28) methyl groups being each refined over three sites, each with equal occupancy; all butyl carbon atoms were refined with individual isotropic thermal parameters. Hydrogen atoms were not included in the model. The refinement was continued with sigma weights until $R = 0.056$ and $R_w = 0.053$; the maximum residual electron density peak in the final difference map was 0.51 e \AA^{-3} . Final fractional atomic coordinates for the nonhydrogen atoms are listed in Table 3 and the numbering scheme employed is shown in Fig. 1 which was drawn with ORTEP [11]. Data manipulation were performed with the TEXSAN program [8] installed on an Iris Indigo work station. Other crystallographic details, comprising thermal parameters, all

Table 2

In vitro antitumour activities (ng ml^{-1}) of $\{[(1,7\text{-C}_2\text{B}_{10}\text{H}_{11}\text{-1-COO})\text{Bu}_2\text{Sn}]_2\text{O}\}_2$, compound **1**, together with those of some reference compounds used clinically against MCF-7 and EVSA-T, two breast cancers, WiDr, a colon cancer, IGROV, an ovarian cancer, M19 MEL, a melanoma, and A498, a renal cancer

Compounds	MCF-7	EVSA-T	WiDr	IGROV	M19 MEL	A498
1	45	38	290	110	110	140
Carboplatin	10 500	4500	3500	2400	5500	18 000
<i>Cis</i> -platin	1400	920	1550	230	780	1200
5-Fluorouracil	350	720	440	850	310	340
Methotrexate	15	26	7	20	18	16
Doxorubicin	25	13	18	150	21	55

bond distances and angles, and tables of observed and calculated structure factors are available on request (ERTT).

Table 3
Fractional atomic coordinates for the nonhydrogen atoms in $\{(1,7\text{-C}_2\text{B}_{10}\text{H}_{11}\text{-1-COO})\text{Bu}_2\text{Sn}_2\text{O}\}_2$

Atom	x	y	z
Sn(1)	0.63613(8)	0.02793(8)	0.56619(9)
Sn(2)	0.43023(8)	-0.25679(8)	0.4533(1)
O(1)	0.4844(6)	-0.993(6)	0.4895(7)
O(2)	0.7239(8)	-0.0815(9)	0.6029(10)
O(3)	0.6084(9)	-0.2391(9)	0.5531(11)
O(4)	0.2657(7)	-0.2467(7)	0.3721(8)
O(5)	0.2055(8)	-0.4226(8)	0.3171(11)
C(1)	0.7000(15)	-0.1708(13)	0.5982(14)
C(2)	0.8025(11)	-0.1968(10)	0.6601(11)
C(3)	0.1884(12)	-0.3415(12)	0.3216(12)
C(4)	0.0638(11)	-0.3509(11)	0.2664(13)
C(5)	0.8723(14)	-0.3389(15)	0.7093(21)
C(6)	-0.0881(15)	-0.2904(17)	0.1371(17)
C(11)	0.6874(11)	0.1020(10)	0.7476(11)
C(12)	0.6392(12)	0.0265(11)	0.7913(13)
C(13)	0.6801(15)	0.911(14)	0.9282(16)
C(14)	0.6367(16)	0.0089(16)	0.9669(17)
C(15)	0.6955(11)	0.0280(11)	0.4385(12)
C(16)	0.6502(14)	-0.0797(14)	0.3426(16)
C(17)	0.6979(17)	-0.0723(16)	0.2514(18)
C(18)	0.6312(20)	-0.1755(20)	0.1409(22)
C(21a)	0.4108(33)	-0.2641(29)	0.6099(32) ^a
C(21b)	0.4172(29)	-0.3106(28)	0.5720(30) ^a
C(22)	0.3208(26)	-0.3043(26)	0.5911(28)
C(23)	0.3223(38)	-0.3377(33)	0.6945(39)
C(24c)	0.3592(58)	-0.2560(53)	0.7891(56) ^b
C(24a)	0.2305(48)	-0.3493(51)	0.6743(55) ^b
C(24b)	0.2744(60)	-0.2741(53)	0.7571(60) ^b
C(25)	0.4317(13)	-0.3450(13)	0.2923(14)
C(26)	0.4453(17)	-0.4512(18)	0.2943(19)
C(27)	0.4473(27)	-0.5214(28)	0.1813(29)
C(28c)	0.5282(46)	-0.5021(50)	0.1583(48) ^b
C(28a)	0.4874(64)	-0.4546(56)	0.1547(60) ^b
C(28b)	0.4344(59)	-0.6145(58)	0.1328(62) ^b
B(21)	0.7961(20)	-0.3213(16)	0.5921(20)
B(22)	0.8842(24)	-0.2142(27)	0.5928(26)
B(23)	0.9354(18)	-0.1023(19)	0.7206(33)
B(24)	0.8721(28)	-0.1322(30)	0.8053(18)
B(25)	0.7790(20)	-0.2838(28)	0.7137(33)
B(26)	1.0029(37)	-0.1288(29)	0.8482(29)
B(27)	1.0208(20)	-0.1623(27)	0.7308(43)
B(28)	0.9366(24)	-0.3026(23)	0.6389(20)
B(29)	0.9159(34)	-0.2363(44)	0.8451(36)
B(30)	1.0095(17)	-0.2518(15)	0.7916(19)
B(41)	0.0442(15)	-0.2339(15)	0.2726(16)
B(42)	0.0178(15)	-0.3408(14)	0.1343(16)
B(43)	-0.0308(15)	-0.4689(15)	0.1425(17)
B(44)	-0.0305(14)	-0.4426(14)	0.2800(17)
B(45)	0.0157(15)	-0.2959(14)	0.3619(17)
B(46)	-0.873(16)	-0.2616(16)	0.2745(18)
B(47)	-0.1318(15)	-0.3879(16)	0.2778(17)
B(48)	-0.1577(15)	-0.4896(17)	0.1489(19)
B(49)	-0.1322(15)	-0.4324(16)	0.0576(17)
B(50)	-0.1925(16)	-0.3798(18)	0.1434(17)

^a Atom has site occupancy factor = 0.5.

^b Atom has site occupancy factor = 0.33.

3.3. NMR experiments

All NMR spectra were recorded in CDCl_3 solutions on a Bruker AC250 instrument, using a QNP probe tuned at 250.13, 62.93, and 93.28 MHz for ^1H , ^{13}C , and ^{119}Sn nuclei, respectively. ^1H and ^{13}C resonances were referenced to the solvent peak at 7.24 and 77.0 ppm, while $\chi(^{119}\text{Sn}) = 37.290665$ [12] was used for the ^{119}Sn resonances. Chemical shifts in ppm and coupling constants in Hz. Abbreviations: t = triplet; tq = triplet of quartet; m = complex pattern; nv: non visible.

3.4. Mössbauer spectra

Mössbauer spectra were obtained as described previously [13]. QS = quadrupole splitting; IS = isomer shift; Γ_1 and Γ_2 = line widths, all in mm s^{-1} .

3.5. Characterisation

Mössbauer: QS: 3.59, IS: 1.38, Γ_1 : 0.93; Γ_2 : 1.00; ^1H NMR: α - & β - CH_2 : 1.37–1.61, m; γ - CH_2 : 1.33 (tq, 7, 7) & 1.36 (tq, 7, 7); CH_3 : 0.89 (t, 7) & 0.92 ppm (t, 7); ^{13}C NMR: C-1: 75.9; C-7: 54.6; CO: 166.9; α -C: 28.6 [$^1J(^{13}\text{C}-^{119/117}\text{Sn})$: nv] & 30.7 [$^1J(^{13}\text{C}-^{119/117}\text{Sn})$: nv]; β -C: 27.0 [$^2J(^{13}\text{C}-^{119/117}\text{Sn})$: 35] & 27.6 [$^2J(^{13}\text{C}-^{119/117}\text{Sn})$: nv]; γ -C: 26.6 [$^3J(^{13}\text{C}-^{119/117}\text{Sn})$: 127] & 26.7 [$^3J(^{13}\text{C}-^{119/117}\text{Sn})$: nv]; CH_3 : 13.5 & 13.6 ppm; ^{119}Sn NMR: δ -207.0 & -205.4 ppm [$^2J(^{119}\text{Sn}-\text{O}-^{119/117}\text{Sn})$: 138].

3.6. In vitro screening

The in vitro tests were performed as described previously [14].

Acknowledgements

We thank Dr. B. Mahieu for the Mössbauer spectra and Mrs. I. Verbruggen for the NMR spectra. We are grateful to Mr. H. J. Kolker, Dr. J. Verweij, Prof. Dr. G. Stoter, Dr. J. H. M. Schellens, Laboratory of Experimental Chemotherapy and Pharmacology, Department of Medical Oncology, Rotterdam Cancer Institute, NL-3008 AE, Rotterdam, The Netherlands, for performing the in vitro tests, and Dr. D. de Vos for financial support. This research was supported by INTAS (contract 93-659), by the Belgian Nationaal Fonds voor Wetenschappelijk Onderzoek (N.F.W.O. grant no. S2/5 CD F198, M.G.), the Belgian Fonds voor Kollektief Fundamenteel Onderzoek (F.K.F.O. grant no. 2.0094.94, R.W.), the Belgian Nationale Loterij (grant nos. 9.0050.90 and 9.0006.93, R.W.), the Russian Foundation for Fundamental Research (grant number 93-03-18654, V.B. & L.E.), and the Human Capital and

Mobility Programme of the European Community (Contract Nr ERBCHRXCT920016). The Australian Research Council is gratefully thanked for support of the X-ray facility (E.R.T.T.).

References

- [1] M. Gielen, A. El Khouloufi, M. Biesemans and R. Willem, *Appl. Organomet. Chem.*, 7 (1993) 119.
- [2] M. Gielen, M. Biesemans, A. El Khouloufi, J. Meunier-Piret, F. Kayser and R. Willem, *J. Fluorine Chem.*, 64 (1993) 279.
- [3] M. Gielen, A. El Khouloufi, D. de Vos, H.J. Kolker, J.H. M. Schellens and R. Willem, *Bull. Soc. Chim. Belg.*, 102 (1993) 761.
- [4] M. Gielen, A. El Khouloufi, M. Biesemans, F. Kayser F and R. Willem, *Appl. Organomet. Chem.*, 7 (1993) 201.
- [5] M. Gielen, M. Bouâlam, A. Meriem, B. Mahieu, M. Biesemans and R. Willem, *Heteroatom Chem.*, 3 (1992) 449.
- [6] E.R.T. Tiekink, *Appl. Organomet. Chem.*, 5 (1991) 1; E.R.T. Tiekink, in S.C. Pandalai (ed.), *Trends in Organometallic Chemistry*, Vol. 1, Council of Scientific Research Information, Trivandrum, India, 1994, in press.
- [7] R.N. Grimes, *Carboranes*, Academic Press, New York, 1970.
- [8] texsan, Single Crystal Structure Analysis Software, Version 1.6, 1993, Molecular Structure Corporation, The Woodlands, TX, USA, 1992.
- [9] N. Walker and D. Stuart, *Acta Crystallogr.*, A39 (1983) 158.
- [10] H.-F. Fan, *R-SAPI88: Structure Analysis Programs with Intelligent Control*, Rigaku Corporation, Tokyo, Japan, 1988.
- [11] C.K. Johnson, ORTEP, Report 5136, 1976, Oak Ridge National Laboratory, TN.
- [12] J. Mason, *Multinuclear NMR*, Plenum, New York, 1987, p. 627.
- [13] M. Bouâlam, R. Willem, M. Biesemans, B. Mahieu, J. Meunier-Piret and M. Gielen, *Main Group Met. Chem.*, 14 (1991) 41.
- [14] M. Gielen, A. Bouhdid, F. Kayser, M. Biesemans, D. de Vos, B. Mahieu and R. Willem, *Appl. Organomet. Chem.*, in press.